Available online at www.sciencedirect.com
SCIENCE DIRECT®
Nuclear Instruments and Methods in Physics Research A 555 (2005) 125–131
NUCLEAR INSTRUMENTS & METHODS IN PHYSICS RESEARCH Section A
www.elsevier.com/locate/nima

Properties of the Ukraine polystyrene-based plastic scintillator UPS 923A

A. Artikov[a,1], J. Budagov[a], I. Chirikov-Zorin[a], D. Chokheli[a,*,2], M. Lyablin[a], G. Bellettini[b], A. Menzione[b], S. Tokar[c], N. Giokaris[d], A. Manousakis-Katsikakis[d]

[a]*Joint Institute for Nuclear Research, Dubna, Russia*
[b]*INFN and University of Pisa, Italy*
[c]*Comenius University, Bratislava, Slovakia*
[d]*University of Athens, Greece*

Received 29 July 2005; received in revised form 12 September 2005; accepted 16 September 2005
Available online 3 October 2005

Abstract

The polystyrene-based scintillator UPS 923A was chosen for upgrading of the muon system for the CDF detector at the Fermilab Tevatron. Properties of this scintillator such as light output, light attenuation, long-term stability and also timing characteristics of scintillators and wavelength-shifting fibers were investigated. The method for the Bulk Attenuation Length measurements of the scintillator to its own light emitted was proposed.

Comparison measurements of the characteristics of the UPS 923A and the polyvinyltoluene-based scintillator NE 114 are done. It was found that natural aging of the NE 114 was two times faster than that of the UPS 923A.

Keywords: Natural aging; Scintillator properties; Polystyrene; Polyvinyltoluene; Light output; Time properties; Technical attenuation length; Bulk attenuation length; Wavelength-shifting fibers

1. Introduction

Plastic scintillation particle detectors are widely used now and will be used in the particle physics experiments. The quality of scintillator detectors is determined primarily by the quality of the scintillating material used by the manufacturer. The scintillator UPS 923A[3] was eventually chosen for upgrading of the muon system for the CDF detector at the Fermilab Tevatron [1]. The bulk material is polystyrene doped with 2% PTP and 0.03% POPOP. This scintillator was used to build about 600 muon counters up to 320 cm long with a novel light collection technique using wavelength-shifting (WLS) fibers [2]. Scintillator properties of light output, light attenuation and long-term stability are investigated. The timing characteristics of scintillators and WLS fibers were also measured.

2. Light attenuation

2.1. Technical attenuation length

The Technical Attenuation Length (TAL) of a plastic scintillator bar is defined as the length reducing the light signal by a factor of e and depending upon bulk transmission of the scintillator, its thickness, shape and reflective properties of the surface. We measured the TAL of the UPS 923A plastic scintillator bar and compared it to the well-known plastic scintillator NE 114.[4] For this purpose, two long scintillation counters with the UPS 923A and NE 114 plastic scintillators viewed by a single photomultiplier (EMI 9814B) at the short side of the bars

*Corresponding author. Tel.: +7 9621 63816; fax: +7 9621 65324.
E-mail address: chokheli@nusun.jinr.ru (D. Chokheli).
[1]On leave from NPL, Samarkand State University, Uzbekistan.
[2]On leave from HEPI, Tbilisi State University, Georgia.
[3]Ukrainian Plastic Scintillator 923A is manufactured by the Institute of Scintillating Materials, Kharkiv, Ukraine.
[4]NE 114 was manufactured by Nuclear Enterprises Ltd. This product is equivalent to BC 416, which is now being manufactured by Bicron Corp.

0168-9002/$ - see front matter © 2005 Elsevier B.V. All rights reserved.
doi:10.1016/j.nima.2005.09.021

through a "fish tail" light guide were built. The scintillator itself was $200 \times 30 \times 2\,cm^3$ bar. To one of its end, a "fish tail" light guide was glued by special optical cement NE 581. The second end was painted black to suppress light reflection. The design of the counters is detailed in Ref. [3].

The properties of the counters were investigated with cosmic muons selected by a telescope of two small scintillation counters ($\approx 4 \times 10\,cm^2$). The counter to be studied was placed between them. Moving the telescope along the counter axis, we measured dependence of the light yield on the distance from the bar edge. A LeCroy ADC 2249A charge-digital converter measured the PMT signal amplitude. The spectrometric channel was calibrated in absolute units, i.e. in the number of photoelectrons created on the PMT photocathode. The calibration was done by means of a fast LED, with the use of low-intensity light flashes. The calibration method and measurements developed by us are detailed in Refs. [3,4].

The results of the measurements are presented in Fig. 1. The TAL was found to be 130 cm for the UPS 923A bar and 115 cm for the NE 114 bar, so they are comparable. One can see that the light yield for the UPS 923A counter is approximately 25% higher than for NE 114.

2.2. Bulk attenuation length

The transparency of the scintillator material is determined by the so-called Bulk Attenuation Length (BAL)–the length which reduces the initial light intensity by factor e according to the Buger–Lambert law. The BAL of the UPS 923A scintillator was measured by means of a cadmium-vapor laser with the 441-nm wavelength and it was found to be about 260 cm.[5]

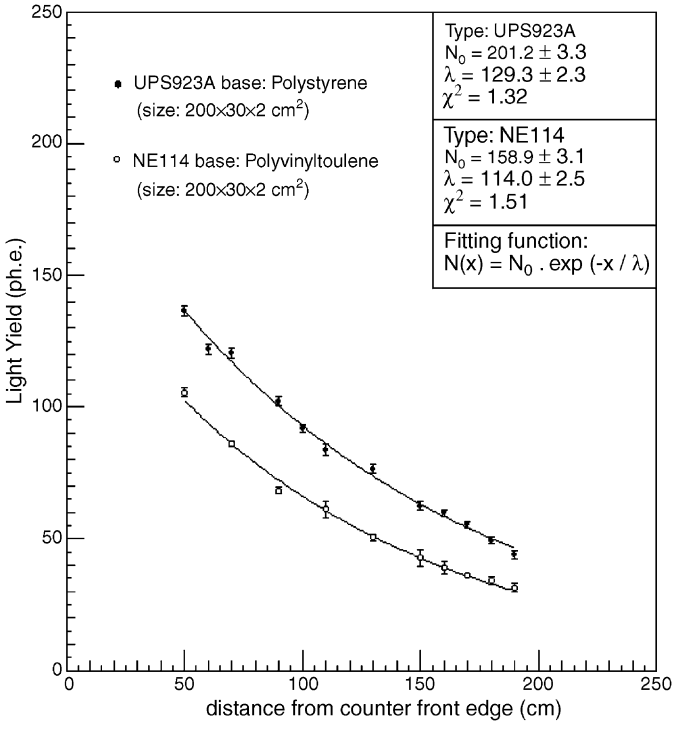

Fig. 1. Light yield of the counters versus the distance from the front end of the scintillator bar.

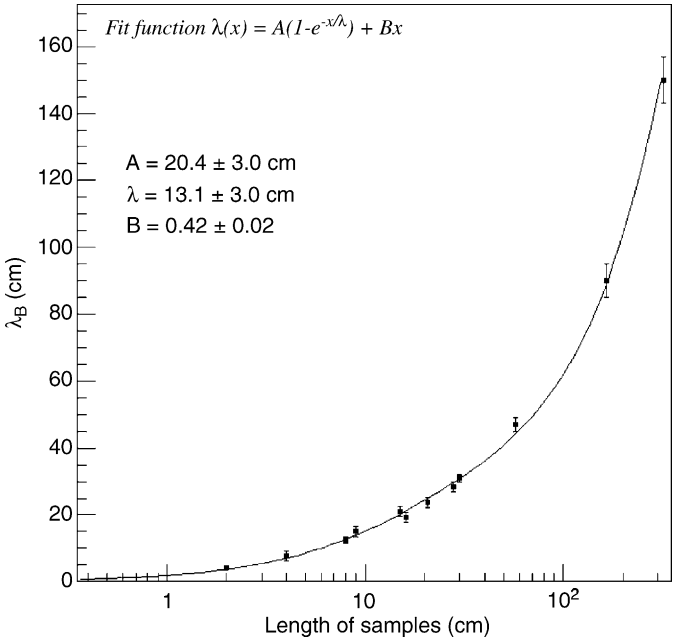

Fig. 2. Dependence of the bulk attenuation length λ_B on the light propagation in the scintillator.

It is important to stress that the main optical parameter of the scintillator material is transparency for its own light emitted.

Measurements of the scintillator BAL for its own light emitted were performed by the parallel beam light with a spectrum which was very close to the emission spectrum of the scintillator (spectrum of the wavelength shifter POPOP) [6]. An ordinary filament lamp was used as a light source. The lamp light spectrum was corrected by light filters "CC5" and "ΦC1" [7]. The resulting spectrum of the parallel beam light was checked by the optical spectrum analyzer.

In the dopant POPOP, the absorption and emission spectrum partly overlap [6]. Therefore, the short-wavelength part (less than about 400 nm) of the emitted light of the scintillator was very rapidly attenuated basically due to the reabsorption effect. Thus, the spectrum of the emitted light is shifted to the long-wave region, where the processes of absorption and reabsorption are less significant [5,8]. In general, therefore, the light attenuation of the scintillator should not exhibit exponential dependence upon the light propagation distance.

To investigate self-absorption, we measured the BAL of a set of scintillator UPS 923A samples with different lengths, which were made from the same scintillation block (Fig. 2).

The experimental data were approximated by the function:

$$\lambda_B = A(1 - e^{-x/\lambda}) + Bx. \quad (1)$$

[5]BAL of scintillator NE 110 for the 458 nm wavelength is 204 cm [5].

Here, the first term describes strong self-absorption of scintillator light in the overlap region. The BAL for the light that traveled less than about 30 cm depends upon the concentration and properties of the fluors, wavelength shifter[6] and material of the scintillator base. The second term describes the region (more than 30 cm) where the short-wavelength wing of the spectrum of emitted light was essentially absorbed and therefore the bulk transmission of the scintillation material is increasing. In this region, the BAL becomes dependent on the quality (purity) of base material and of dopants.

3. Time response properties of the scintillator and WLS fibers

The scintillator detector time resolution is determined primarily by the shape of the light pulse excited by a particle in the scintillator and also by the time properties of WLS fibers used in the optical read-out system.

The light pulse shape studies were performed by the single-photon method of Bollinger and Thomas [9]. Fig. 3 shows a simplified block diagram of the time spectrometer we invented for decay time study. Samples (S) were disks 15 mm in diameter and 1.5 mm thick with polished surfaces. The samples were excited by electrons from a ^{106}Ru + ^{106}Rh source with the maximum energy 3.54 MeV. To improve the time resolution of the setup, a Cherenkov counter was used to generate a trigger signal. The Cherenkov radiator cylinder 9 mm in diameter and 6 mm high was made of quartz. The radiator was coupled to the Hamamatsu H6780-06 photosensor (sensitive in ultraviolet region) by optical grease RHODORSIL SI 200. The Cherenkov counter signal is discriminated by the leading edge discriminator (D) and an output signal was used to start a LeCroy 2228A TDC.

The H5783 photosensor was used to detect the single photon from the edge of the samples. The photon counter was tuned to the single-photon mode with the help of an iris diaphragm (ID), which reduced the detected signal to approximately 0.01 photoelectrons on an average. Such radiation attenuation is needed to maintain the probability of detection of two or more photoelectrons in one light pulse at a negligibly small level ($<10^{-4}$). The single-photon signal from H5783 is discriminated by a constant fraction discriminator (CFD) and an output signal is used to stop the TDC.

The time resolution of the system for the single photoelectron was measured with a lucite sample which yields fast Cherenkov light signals. Since the light from the Cherenkov process is emitted essentially instantaneously and the light output was limited to a single photoelectron, the measured time distribution is a direct measure of the system response (apparatus function). Fig. 4 shows a typical Cherenkov time distribution.

[6]The scintillator with a large Stokes shift wavelength shifter has a comparatively small self-absorption of its emitted light [6].

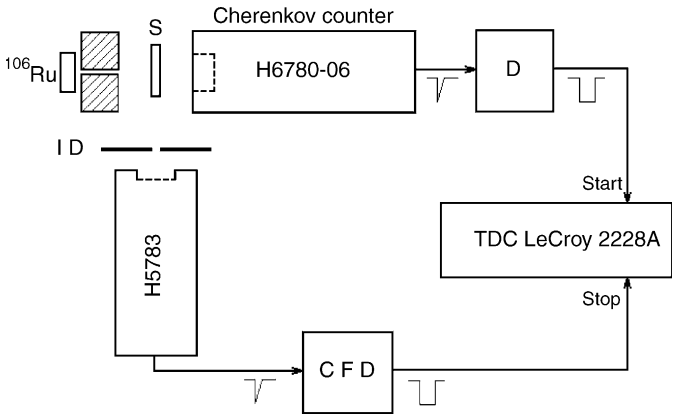

Fig. 3. Experimental setup for decay time measurements.

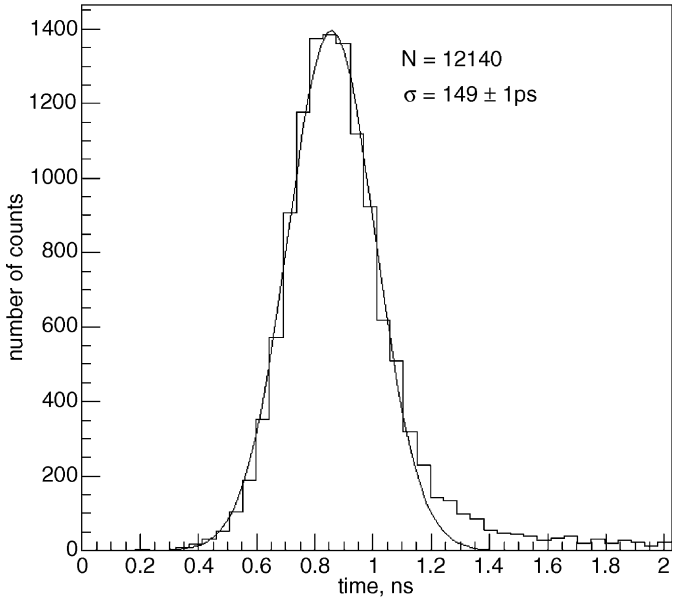

Fig. 4. Apparatus function measurement with Cherenkov light.

In the Gaussian approximation, the measured system resolution is $\sigma \approx 150$ ps.

Many processes contribute to the scintillation light emission [10,11]. The light pulse shape $f(t)$ from plastic scintillators can be described as consisting of a fast component generated by the two-step scintillation cascade and an additional slow component; with these assumptions, $f(t)$ is expressed as follows:

$$f(t) = \frac{N}{1+R}\left[\frac{e^{-t/\tau_2} - e^{-t/\tau_1}}{\tau_2 - \tau_1} + R\,\frac{e^{-t/\tau_3}}{\tau_3}\right] \quad (2)$$

where N is the total number of photons, τ_1 the rise time constant, τ_2 the decay time constant of the fast scintillation process, τ_3 the decay time of the slow component and R is the ratio of the light components produced through the slow and fast decay processes.

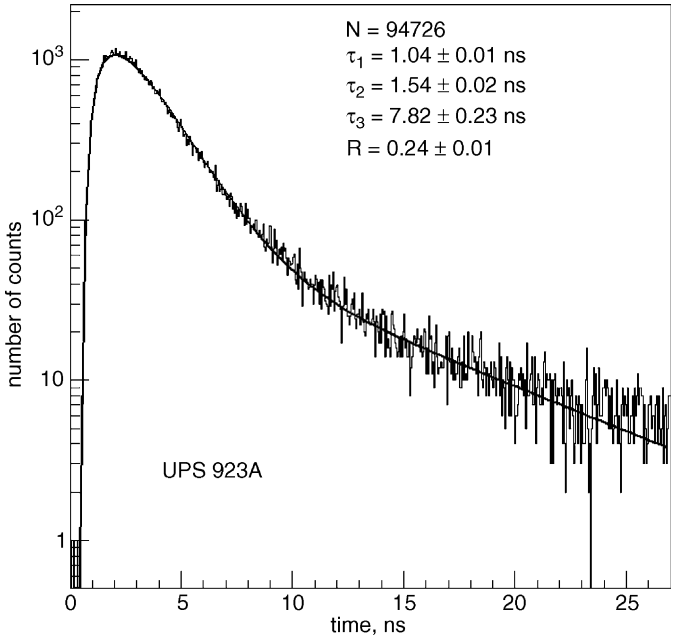

Fig. 5. Time distribution spectrum of the light pulse from the UPS 923A scintillator sample.

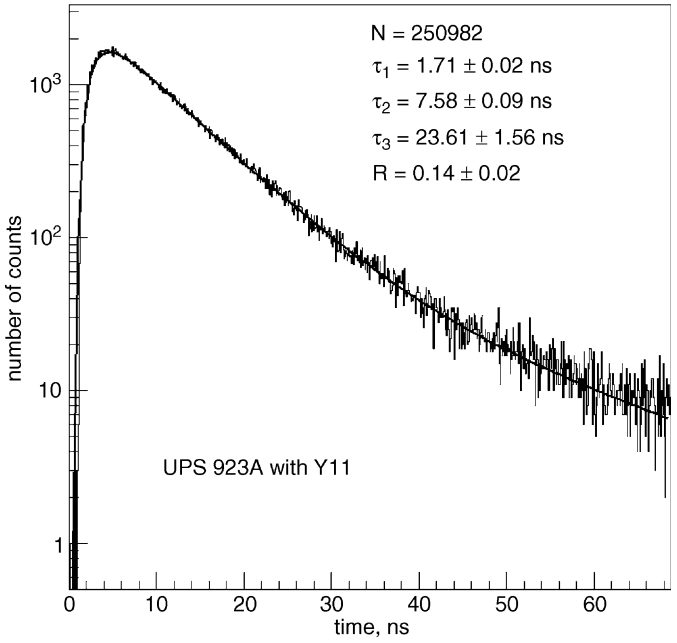

Fig. 6. Time distribution spectrum of the light pulse from the UPS 923A sample with Y 11(250) MS fibers.

Fig. 5 shows the time spectrum of the light pulses of the UPS 923A scintillator. The measured time distribution is described by the convolution integral of expression (2) and the Gaussian apparatus function (Fig. 4). But in our case, the time resolution of the system for single photoelectrons (FWHM $\approx$ 350 ps) is significantly smaller than the scintillation pulse duration. Therefore, in the first approximation, the spectrum was fitted by formula (2). A comparison of

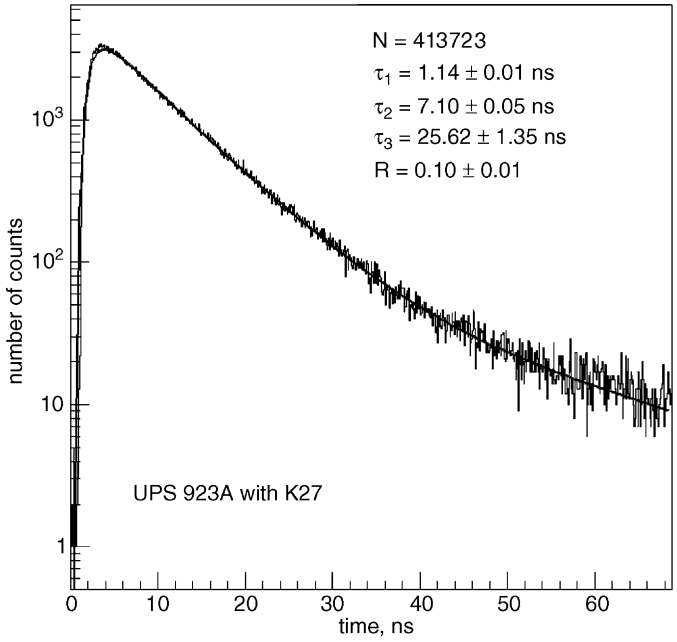

Fig. 7. Time distribution spectrum of the light pulse from the UPS 923A sample with K 27(200) MS fibers.

the measured time distribution with the results of the fit is shown in Fig. 5.

We have studied the time response of WLS fibers. For this purpose, the samples of the scintillator UPS 923A were coupled to WLS fibers with optical glue. Figs. 6 and 7 present the time spectrum of the light pulse from UPS 923A with WLS fibers. The time spectra were also fitted by phenomenological formula (2).

To conclude, we list the main useful time parameters of light pulse shapes of the scintillator and WLS fibers: rise time (level 0.1–0.9), fall time (level 0.9–0.1), FWHM (level 0.5–0.5) and pulse duration (level 0.1–0.1), as given in Table 1. The parameters of the Cherenkov light pulse from the lucite samples are given in Table 1 as well. It is important to note that the rise time of the light pulses from the scintillator UPS 923A with WLS fibers is fast ($\approx$2 ns), therefore counters with WLS fibers read-out can be used in fast coincidence systems and time-of-flight measurements.

4. Long-term stability

Natural scintillator aging depends on the components used. We have investigated natural aging of the plastic scintillator UPS 923A based on polystyrene (PS) and compared it to a well-known product NE 114 based on polyvinyltoluene (PVT). For these studies, two long scintillation counters with the UPS 923A and NE 114 plastic scintillator were built. The design of the counters and the measurement methods are described in Section 2.

Measurements of the counter light yield were done in December 1992 and November 1996. The results are summarized in the following figures. In Figs. 8 and 9, we

Table 1
Measured time parameters of the light pulse shapes

Material	Rise time (ns) (level 0.1–0.9)	Fall time (ns) (level 0.9–0.1)	FWHM (ns) (level 0.5–0.5)	Pulse duration (ns) (level 0.1–0.1)
UPS 923A	0.8	5.3	3	7.2
UPS 923A + K27	1.7	17.3	7.8	19.1
UPS 923A + Y11	2.2	18	8.8	22.4
Lucite	0.23	0.23	0.33	0.65

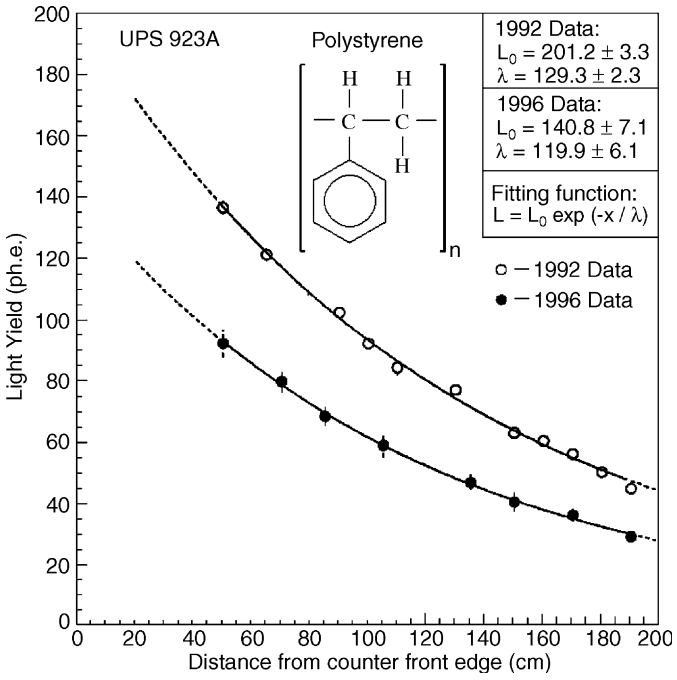

Fig. 8. Light yield of the PS-based scintillator (UPS 923A) counter versus the distance from the front end of the bar. Measurements were done in 1992 and 1996.

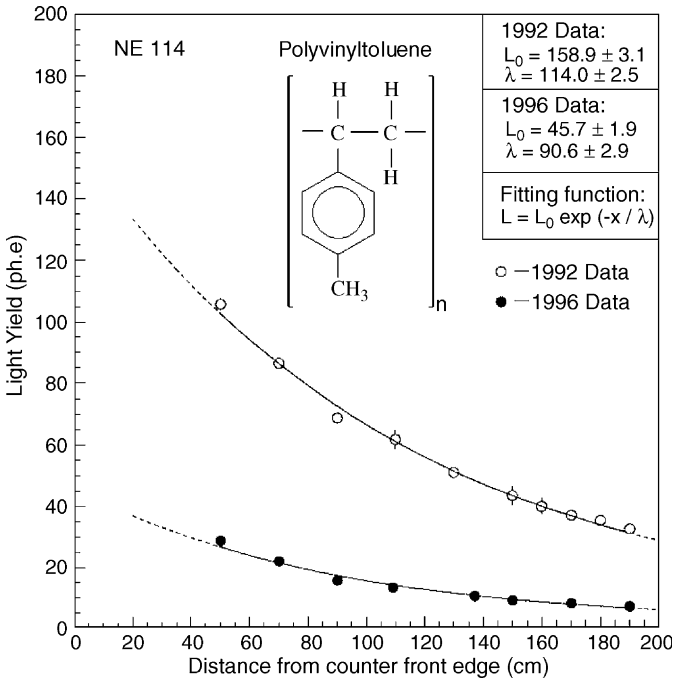

Fig. 9. Light yield of the PVT-based scintillator (NE 114) counter versus the distance from the front end of the bar. Measurements were done in1992 and 1996.

give the light yield as a function of the distance from the front-end scintillator bars for the UPS 923A and NE 114 counters respectively. For comparison, we fitted the corresponding light yield with the single exponential function ($L = L_0 e^{-x/\lambda}$). As one can see in Figs. 8 and 9, for 4 years, the UPS 923A scintillator light yield decreased by ≈30% (≈7.5%/year), while the scintillator light of NE 114 decreased by ≈70% (≈18%/year). Thus, natural degradation of the light yield of the NE 114 scintillator bar is more than two times faster than that of the UPS 923A scintillator bar.

Visual inspection revealed that the NE 114 scintillator bar got a yellow–green color in contrast to the Ukrainian UPS 923A scintillator bar which remained quite blue. The ensuring investigation led to the discovery that over the 8 years' period, the scintillator NE 114 had deteriorated to the degree that when exposed to daylight, the scintillator for emitted light visibly shifted to the green, and measurements revealed that the transmission had indeed decreased by 1%/ cm between 400 and 500 nm where most of the scintillator emission occurs [12].

The polymeric bases of the PVT and PS scintillator bars have different chemical structure. This difference is determined by the fact that in PVT, unlike the case in PS, a methyl group (–CH_3) substitutes for one hydrogen atom in the benzene ring (see Figs. 8 and 9).

Processes resulting in both chemical and physical structure degradation occur in the polymeric base with time. It is manifested in the appearance of dotty defects on the surface and in the bulk of the scintillator bars, as well as microvoids, cracks known as "silver" and minute cracks.

Originally, three types of free radicals are possible to appear in PVT under the effect of external destabilization factors such as temperature, UV light, oxygen, humidity and external radiation:

(1) a tertiary methylbenzene radical is created by tearing off the tertiary atom of hydrogen,
(2) a primary benzene radical is created by tearing off a hydrogen atom from the methyl group,
(3) a benzene radical is created by tearing off the methyl group.

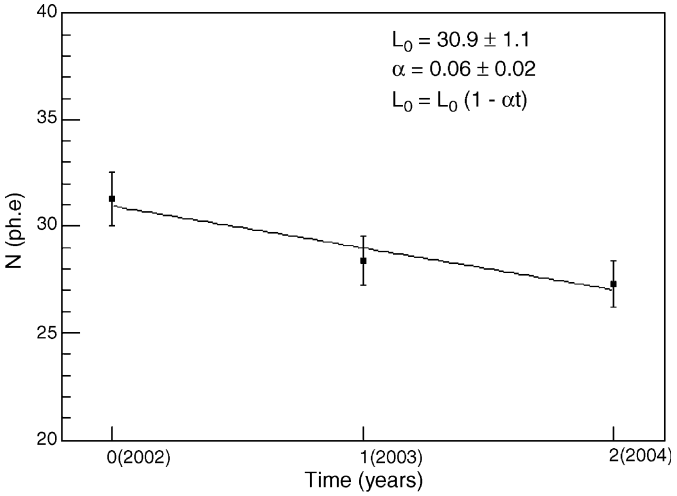

Fig. 10. Dependence of the light yield in terms of the photoelectron per MIP on time for the 320-cm-long counter.

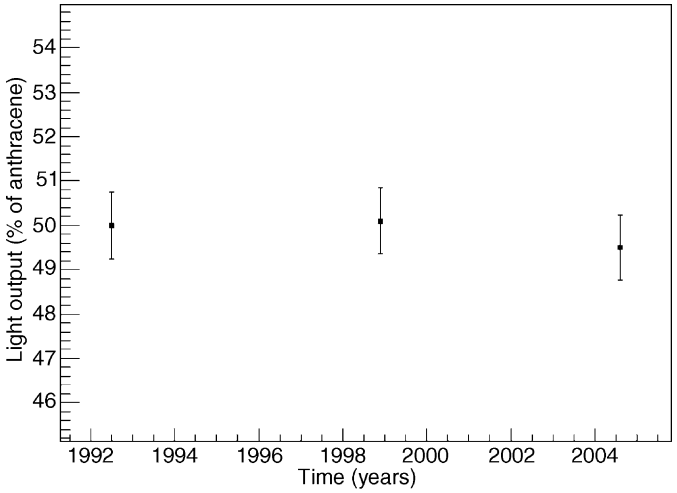

Fig. 11. Light output of the small sample in percent of anthracene as a function of time.

In the PS case, only one type of free radical is originally generated—a tertiary benzene radical resulting from tearing off the tertiary atom of hydrogen.

As known, each of the free radicals created under effect of oxygen and other external factors can initiate the polymeric degradation process, in particular the oxidation chain process. Hence, the probability for degradation processes to begin and their velocity in PVT will be several times higher than in PS, and this difference was for the first time observed by us as described above.

We also investigated the light yield deterioration of the 320-cm-long counter with the WLS fiber read-out [2] for the period of 2001–2004. Fig. 10 shows dependence of the light yield in terms of photoelectrons per MIP on time. The signal was measured 30 cm away from the front end of the scintillator counter. In order to survey the long-term stability of the observed light yields, they were fitted as a linear function of time:

$$L = L_0(1 - \alpha t). \quad (3)$$

Here, L_0 is the fit parameter which corresponds to the observed light yield at the time of the first measurement and α is the variation rate of the observed light yield. The change in the observed light yield was estimated at a level of about 6% per year.

In order to evaluate the natural degradation of light output of the scintillator UPS 923A, we performed parallel light yield measurements with a small sample over the 12 years' period. The scintillator sample was a disk, 16 mm in diameter and 10 mm thick with polished surface. The sample of the scintillator was stored in a dark place over the entire investigation period. The light yield measurements were carried out by using a radioactive ^{137}Cs source for excitation. The sample was placed directly (without optical grease) at the center of the EMI 9814B PMT window and the pulse height conversion electron spectrum of ^{137}Cs ($E_e = 624$ KeV) was measured. Light yield is measured relative to a reference sample whose light output was calibrated in percent of anthracene. The results of our investigation are presented in Fig. 11. We did not observe natural degradation of the scintillator UPS 923A light output over the 12 years' period.

The scintillation efficiency (light output) degradation is first of all defined by the degree of luminescent dopant (LD) damage. The LD used in the UPS 923A scintillator were POPOP and PTP, which have much smaller thermal and thermooxidation destruction than the PS base [13].

In conclusion, note that natural scintillation aging is mainly defined by destruction of the polymeric base.

5. Conclusion

We have investigated the characteristics of the PS-based scintillator UPS 923A and compared some of them with the PVT-based scintillator NE 114. The TAL of the UPS 923A and NE 114 scintillator bars with dimensions $200 \times 30 \times 20\,\text{cm}^3$ are comparable. According to the Buger–Lambert law, the BAL of the scintillator UPS 923A for the wavelength 441 nm is about 260 cm.

The method for the BAL measurements of the scintillator for its own light emitted was proposed. It was found that the BAL of the scintillator UPS 923A for its own light emission is not a constant value and strongly depends on light propagation in the scintillator due to reabsorption effect.

The rise time of the scintillator UPS 923A light pulse is less than 0.8 ns and the rise time of the light pulse of "the UPS 923A plus the WLS fibers" couple is about 2 ns. Therefore, scintillation counters with the WLS fiber read-out can be used in fast coincidence systems to observe rare particles against large background of other events and in time-of-flight measurements.

We found out that natural degradation of the light yield of the PVT-based scintillator NE 114 bar is more than

twice faster than that of the PS-based scintillator UPS 923A bar.

It is also essential that no natural degradation of the scintillator UPS 923A light output was observed over 12 years.

References

[1] The CDF-II Detector Technical Design Report. The CDF II Collaboration, Fermilab-Pub-96/390-E, 1996 (Chapter 10).
[2] A. Artikov, et al., Nucl. Instr. and Meth. A 538 (2005) 358.
[3] E.H. Bellamy, et al., Nucl. Instr. and Meth. A 343 (1994) 484.
[4] E.H. Bellamy, et al., Nucl. Instr. and Meth. A 339 (1994) 468.
[5] G. Kettenring, Nucl. Instr. and Meth. 131 (1975) 451.
[6] P. Destruel, et al., Nucl. Instr. and Meth. A 276 (1989) 69.
[7] A.H. Zaidel', G.V. Ostrovkaya, Yu.I. Ostrovskii, Tekhnika I praktika spektoskopii, Fizika I tekhnika spektral'nogo analiza (Biblioteka injenera). Izdatel'stvo "Nauka", 1976 (in Russian).
[8] J. Kirkby, Today and tomorrow for scintillating fibre (SCIFI) detectors, CERN-EP/87-60 (1987).
[9] L.M. Bollinger, G.E. Thomas, Rev. Sci. Instr. 32 (1961) 1044.
[10] J.B. Birks, J. Phys. B1 (1968) 946.
[11] E.N. Matveeva, et al., Nucl. Instr. and Meth. 179 (1981) 277.
[12] S. Cabrera, et al., Nucl. Instr. and Meth. A A453 (2000) 245.
[13] V.G. Senchishin, N.B. Verezub, S.N. Lavrienko, Technologia proizvodstva polimernikh opticheskikh izdelij, Kiev, Technika, 1992, str. 68 (in Russian).